been inspired by the new information of Early Tertiary faunas outside the Rocky Mountain region. Nevertheless, the abundance of contradictory scenarios, as well as shortcomings of age correlations (*14*), indicate the ambiguity or absence of the faunal data for dispersal events. A century of empirical studies support the synchrony of faunas that characterize land mammal ages and the temporally discrete nature of these ages. Therefore, closely similar faunas must be regarded as roughly contemporaneous unless there is clear, independent evidence to the contrary. Complicated scenarios for dispersal of Wasatchian vertebrates are unjustified, at least until we have an established independent geochronology and much better data on the geography of faunal succession for the late Paleocene and early Eocene of Holarctica.

JOHN J. FLYNN

Department of Geological Sciences, Rutgers University, New Brunswick, New Jersey 08903

MICHAEL J. NOVACEK

Department of Vertebrate Paleontology, American Museum of Natural History, New York 10024

References and Notes

1. H. E. Wood II *et al.*, *Geol. Soc. Am. Bull.* **52**, 1 (1941).
2. L. J. Hickey, R. M. West, M. R. Dawson, D. K. Choi, *Science* **221**, 1153 (1983).
3. R. F. Butler, P. D. Gingerich, E. H. Lindsay, *J. Geol.* **89**, 229 (1981). Butler and Lindsay (but not Gingerich) suggested a temporal overlap of Torrejonian and Tiffanian (Paleocene) faunas from Wyoming and New Mexico but rejected this because of new magnetostratigraphic evidence [*Eos* **64** (No. 45), 683 (1983)].
4. K. D. Rose, *Science* **208**, 744 (1980); *Univ. Mich. Pap. Paleontol. 26* (1981).
5. P. D. Gingerich, K. D. Rose, D. W. Krause, *Univ. Mich. Pap. Paleontol. 24* (1980), p. 51; P. D. Gingerich and R. A. Haskin, *Contrib. Mus. Paleontol. Univ. Mich.* **25** (No. 17), 327 (1981); P. D. Gingerich, *J. Mammal.* **63**, 488 (1982); P. D. Gingerich and G. F. Gunnell, *Contrib. Mus. Paleontol. Univ. Mich.* **25** (No. 7), 125 (1979).
6. R. G. Gastil, R. P. Phillips, E. C. Allison, *Geol. Soc. Am. Mem. 140* (1975). The designation "Lomas las Tetas de Cabra" is given in Hoja Rosarito (1977), Comision de Estudios del Territorio Nacional.
7. W. J. Morris, *Science* **153**, 1376 (1966); *Contrib. Sci. L.A. County Mus. 151* (1968); I. Ferrusquia-Villafranca, *Univ. Nac. Auton. Mex. Inst. Geol. Bol. 101* (1978), p. 193.
8. The identity and distributions of the nonmammalian vertebrate taxa were provided by R. E. Estes (personal communication); for a description of these taxa and the mammals see J. Flynn, M. J. Novacek, and R. Estes, in preparation. Distributions of Clarkforkian nonmammalian vertebrates were also provided in W. S. Bartels [*Univ. Mich. Pap. Paleontol. 24* (1980), p. 73]. Pre-Clarkforkian occurrences of Iguanidae and cf. *Saniwa* reported by R. M. Sullivan [*J. Paleontol.* **56**, 996 (1982)] are questionable, but material possibly referable to *Saniwa* is known from the type Clarkforkian (R. Estes, personal communication).
9. S. D. Rapp, B. J. MacFadden, J. A. Schiebout, *J. Geol.* **91**, 555 (1983). *Hyracotherium* is reported from Big Bend, Texas, in a reversed interval between magnetic anomalies 24 and 25. The occurrence was tentatively given a Clarkforkian age, but comparisons with Big Horn Basin faunas indicate a possible Wasatchian correlation. The Tiffanian (late Paleocene) occurrence of *Hyracotherium* reported by G. L. Jepsen and M. O. Woodburne [*Science* **164**, 543 (1969)] is unsubstantiated (*4*).
10. R. E. Sloan, *Proc. North Am. Paleont. Conv.* **1(E)**, 427 (1969).
11. P. D. Gingerich, *Univ. Mich. Pap. Paleontol. 15* (1976).
12. M. Godinot, *Palaeovertebrata* **10-II**, 43 (1981); *Geobios Mem. Spec.* **6**, 403 (1982).
13. Godinot (*12*) argued that several taxa from France in addition to *Plesiadapis* were more primitive, and thus older, than congeneric North American species.
14. Only two recent studies (*2, 3*) propose heterochrony for a given North American land mammal age on the basis of independent geochronologic evidence. The magnetostratigraphic evidence for the temporal correlations of Hickey *et al.* (*2*) is poorly documented and does not provide an independently defined geochronology (D. V. Kent, M. C. McKenna, N. D. Opdyke, J. J. Flynn, B. J. MacFadden, *Science*, in press). Revision of the Butler *et al.* study (*3*) now provides strong support for the synchrony of a particular North American land mammal age.
15. C. G. A. Harrison and T. Lindh, *J. Geophys. Res.* **87** (B3), 1903 (1983).
16. We gratefully acknowledge the cooperation of Instituto de Geologia, Mexico City. We thank A. Wyss, R. Estes, M. C. McKenna, L. Flynn, R. H. Tedford, and two anonymous reviewers for helpful comments. Fieldwork and research were supported by the Frick Laboratory Endowment, American Museum of Natural History.

1 December 1983; accepted 6 February 1984

Topography from Single Radar Images

Abstract. *A mathematical theory and a corresponding numerical procedure have been developed to produce digital topography from radar images as digital photometric arrays. Thus, as radargrammetry is to photogrammetry, so radarclinometry is to photoclinometry. Photoclinometry encompasses a fundamental indeterminacy principle even for terrain that is homogeneous in normal albedo, because the surface normal consistent with a given reflected specific intensity is not unique. A geometric locus of such normal directions is implied, which generates a surface. For microwave backscatter, in specific application to radarclinometry, this surface is a cone whose half-angle is the incidence angle, whose axis contains the radar, and whose apex coincides with the terrain point. Although the indeterminacy can be removed if a properly directed profile of ground truth is available as a constraint, such is seldom the case. In its absence, an auxiliary assumption, such as that the strike line runs perpendicular to the illumination line, is needed. If metric integrity is a goal, then this is an absurd assumption. Herein, "the hypothesis of local cylindricity" has been assumed, a premise regarding the nature of topographic curvature that seems more realistic and that makes possible the production of topography as a set of parallel line integrals.*

When the Venus Radar Mapper orbits the perennially beclouded cytherean globe later in this decade, the first opportunity will present itself for high-resolution mapping of her surface. It is hoped that the data products of this mission will include topographic maps with a resolution comparable to that of the radar images. The capacity for obtaining such results by the necessary target date is not a foregone conclusion. Application of the traditional methods of photogrammetry to parallactic pairs of radar images presents serious practical problems because of the peculiar nature of radar images. Studies of such problems are presently under way.

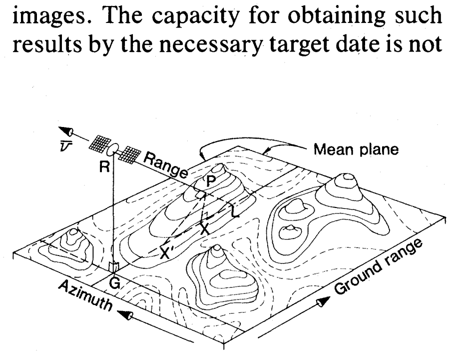

Fig. 1. Illustration of radar image formation. The solid elevation contours lie above the mean plane of the topography; the dashed contours lie below the mean plane. The dashed portions of straight lines lie below the terrain surface. Point P is an arbitrary point of terrain. Its range from the radar is $\overline{RP}$; $\triangle RGL$ and all its interior triangles are right triangles; $\overline{PX}$ is the topographic height; $\overline{X'X}$ is the ground-range mapping distortion of the radar image; and $\bar{v}$ is the orbital velocity. Azimuth, as defined by radar engineers, is a rectilinear coordinate and not be confused with the angle familiar to astronomers and surveyors.

In a parallel effort toward maximizing the probability of attaining this goal, I have developed an operational theory for determining topography from a single radar image rather than a stereometric pair. The method is thus not based on the paralactic depth perception implied, albeit in a peculiar way, by images of the same terrain formed when the radar is in two different orbital revolutions. Nor is it based on a depth perception deriving in any direct way from the fundamental range-finding characteristic of radar. The method, which I call radarclinometry (*1*), is photometric or, in deference to the long wavelength, radiometric in nature.

The radar reflectance of a surface element corresponding to a particular image pixel depends not only on the chemical and microphysical state of the surface but also on the incidence angle, the angle between the local direction to the radar and the local direction perpendicular to the terrain surface. If it can be assumed that the radar ephemeris and antenna orientation are known, and that the terrain encompassed by the format of a radar image is homogeneous in radar microproperties and is also extended enough that the mean plane of the topography (least-squared fit of a plane to the actual topography) is perpendicular to the local vertical, then the only nontrivial relation left to be developed is between the microwave energy represented by the value of an arbitrarily chosen image pixel and the corresponding terrain orientation (*2*). To know the set of unit vectors everywhere perpendicular to terrain is effectively to know the gradient of the height as a function of the image coordinates, from which topographic height itself emerges as a set of line integrals that originate at a common point and terminate at every desired mapping point. However, a fundamental indeterminacy principle inhibits radarclinometry. To know the surface brightness (*3*) of reflected radar radiation from a point of terrain is not to know the local direction of the surface normal, but merely that it is one of many possible directions characterized by the straight lines whose geometric locus forms a cone with its apex at the point of terrain and the radar lying on its axis of symmetry. To know the surface brightness is to know the half-angle of this cone (*4*). The most important contribution of the present study lies in producing a method for selecting a particular direction from this ambiguous set, for each point of terrain corresponding to an image pixel, achieved by adopting the hypothesis of local cylindricity. This assumption will be detailed later in this report.

Inasmuch as radiometrically calibrated radar is a requirement of any method that deals with a digital radar image as a photometric array, it must be candidly admitted that no such thing has existed up to the present time. Radarclinometry requires radar calibration to the point of producing pixel signals that are directly proportional to the microwave energy integrated into each pixel. An accurate constant of proportionality is not needed because a scale factor can be found that forces the mean plane of the derived topography to be perpendicular to the mean vertical. In effect, therefore, a scaling of pixel signal directly into the radar reflectance function (back-scattering cross section versus incidence angle) is achieved, so that that function also need not be known with an absolute physical scale for specific intensity. I do not wish to trivialize the decision regarding the selection of the particular reflectance function that should be used in a specific case, but there is the further mitigating circumstance that a large part of the variation of pixel energy with terrain surface orientation arises from a geometric factor relating this energy to the specific intensity; this factor is canonical, unlike the reflectance function itself (*4*). In any event, until calibrated radars exist, the question remains academic. This report presents a definite plea that the radar in orbit about Venus be radiometrically calibrated. The first radiometrically calibrated radar can be expected to be Shuttle Imaging Radar-B, which will certainly predate the Venus Radar Mapper.

The presentation of a theoretical justification of radarclinometry that is a priori to demonstrated utility is not an objective of this report (*5*). I present here the results of a preliminary application of the new theory, and I describe the theory insofar as it is of contingent interest. The form of scientific justification herein presented may be considered a posteriori.

A delay in methodological development pending the development of calibrated radars would have been foolish, of course; but, in view of the status of such radars, one asks the nature of "results of application" presently possible. To be sure, topographic maps of genuine metric integrity cannot yet be produced, but by heuristically linearizing the relation between output radar signal (even if it is a photographic density measured in an analog-produced radar image!) and pixel energy and assuming a quite nominal curve for the radar reflectance function (*6*) over the range of incidence angle to be found, a geologically useful result has been produced.

The geologic interpretation of surficial expression of terrain through radar images has been widely inhibited by the radar-peculiar distortion that foreshortens the extent of terrain sloped toward the radar and elongates terrain sloped away from the radar, especially in an image that "appears" otherwise to be an orthographic projection in the vertical direction. The problem is illustrated in Fig. 1, where P is a point of terrain reflecting radar energy. For a sufficiently distant radar, the line PX' is contained within a single radar wave crest, so that

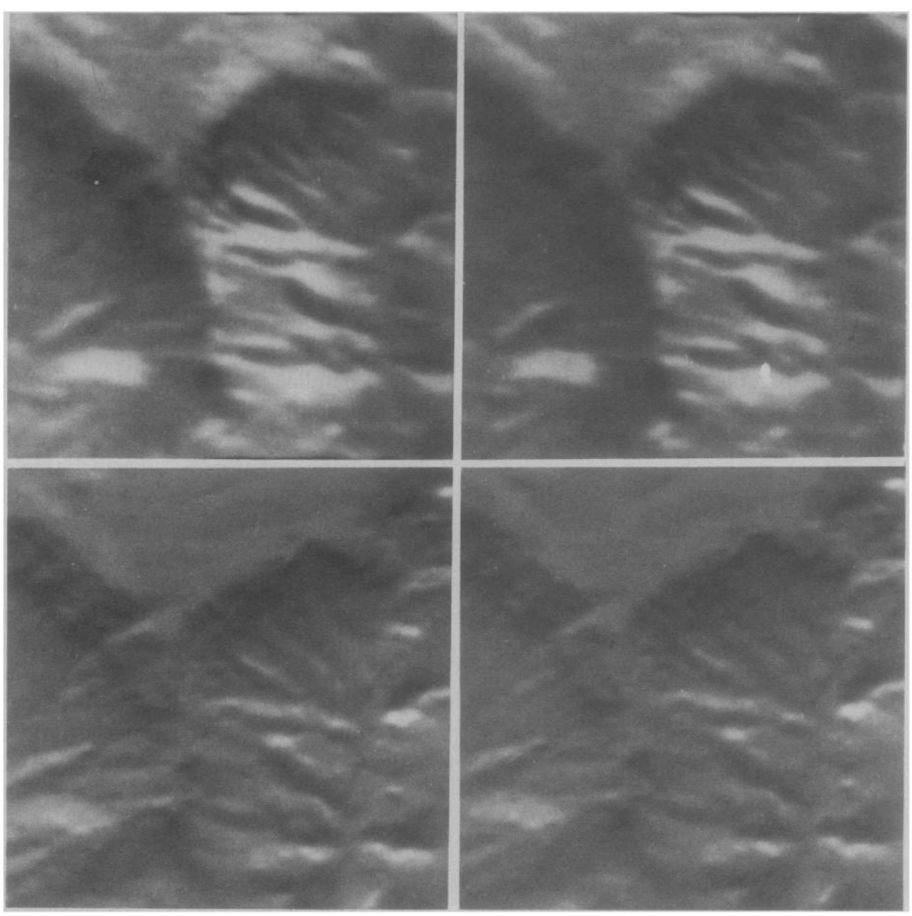

Fig. 2. Shaded-relief stereopairs produced from digitized topography. The topography providing the upper pair was derived radarclinometrically from a single radar image (Motorola side-looking aerial radar). For comparison, the lower pair was derived by digitizing the standard topographic map of roughly the same region (Crazy Jug Point in the Grand Canyon, Arizona) at approximately the same resolution. The effective elevation angles of the artificial sun used to produce the shaded relief differ because the mean plane of the topography for the upper pair tilts relative to the plane of mean sea level characterizing the lower pair.

P and X' have the same radar range time. The point X' lies in the mean plane of the topography and is more nearly where the energy from P will be mapped in the resulting radar image than point X, which represents the mapping of P in a true orthographic projection. The line PX represents the height of the terrain point above the mean plane. If this height is known, the terrain point P can be remapped from X' to X. Such a distortion correction, even if based on a digital topographic file known to possess systematic errors, has been found to facilitate geologic interpretation of radar images (*7*).

In addition to the foregoing consideration, the use of purely heuristic topographic files, derived pseudophotoclinometrically for the purpose of synthesizing subjective stereo pairs, has been found to aid the geologic interpretation of ordinary images acquired in the visual spectral region (*8*). Such an application is also possible for radar images acquired with uncalibrated radar.

The kind of topographic product indicated above is what is presented in this report. The theory used, although presently unmatched by the quality of data, is designed to provide the closest possible approach to the metric integrity obtainable from traditional photogrammetry. To that end, the resolution of the fundamental problem of photoclinometric indeterminacy is crucial. I next examine how that comes about by describing step-by-step the integration process that distributes topographic height over the mean plane. Let us begin by picking a starting point in the radar image that is at the near-range edge. This starting pixel is assigned a height of zero relative to the mean plane. A best estimate of the local orientation of the strike line (a line of zero height change with respect to which the terrain surface normal must be perpendicular) within the mean plane is made for this element. This strike-line orientation resolves the ambiguity in how the two slope components of the terrain, one along ground range and the other parallel to the orbital track (azimuth, in radar nomenclature), shall be chosen to produce the necessary incidence angle consistent with the exhibited magnitude of the image pixel. This approach to the indeterminacy, which is user-dependent, is used only to start the integration process. The information now at hand enables us to step to the adjacent pixel downrange, thereby determining both the height and the mapping coordinates for a vertical projection onto the mean plane of the corresponding terrain element.

With the completion of the first integration step, we are not yet ready to repeat the process at the second pixel. We must first find out how the strike-line orientation has changed from the first pixel position to the second. To do this, we must investigate the surface curvature of the terrain in the vicinity of the first pixel. Since the surface curvature represents the manner by which the local surface normal is changing direction as one shifts position on the surface, it directly determines the brightness gradient in the image. We can measure the brightness gradient in the image. But when we attempt to determine from it the curvature, in the inverse problem, we find that, although the brightness gradient has two independent components as a vector in the image, the terrain surface curvature has three, in the form of the three second partial derivatives of height with respect to horizontal coordinates. It is at this point that the assumption of a locally cylindrical nature of the curvature must be invoked. This assumption provides an additional constraint, which removes the independence of the three components of curvature, rendering them determinate. The axial alignment of local cylindricity, which is generally not parallel to the mean plane, need not be specified a priori. The image pixel brightness and brightness gradient are deterministic of this alignment. The axial direction's projection into the image plane can be measured because it must be the local direction of the image isophote. Its true three-dimensional alignment can then be inferred because the local strike and dip (equivalent to the local unit normal vector) of the terrain are already known. This leaves only the magnitude of the curvature, which is now reduced to a one-to-one correspondence with the magnitude of the image brightness gradient.

With the curvature fully specified, a range integration step can be taken which establishes both the azimuthal and downrange component of slope at the next pixel in the image line. This information is used only to rotate slightly, in a horizontal plane, the strike line that will apply at the next integration step of the topography.

The above process is recycled repetitively to the end of the range line (actually the range-line pair needed to acquire the brightness gradient). As we now shift in azimuth by one range line in order to repeat the entire procedure and thus begin development of topography as a surface rather then merely a curve, we note that the slope and curvature information developed at the beginning of the preceding range-line integration is sufficient to give us starting values for height, coordinates on the mean plane, and strike-line orientation. This process also repeats itself, progressing in azimuth. Thus from the starting point in the image, there is a fully deterministic height profile development to any arbitrary point in the image that proceeds along the azimuthal coordinate of the image and then perpendicularly along the ground-range coordinate of the image. The remapping is simultaneously effected.

The application of radarclinometry to a Motorola radar image of the region of Crazy Jug Point in the Grand Canyon of Arizona is shown in Fig. 2. The radarclinometry first generated a digital file of vertical height of terrain as a function of Cartesian coordinates on the mean plane. To this an algorithm (*9*) was applied, which generated a shaded relief image. A subsequent algorithm (*10*) generated a stereo mate to this image. For comparison, the same products were generated from a hand-digitized height file at roughly the same resolution for the same region as displayed on the standard U.S. Geological Survey–U.S. Coast and Geodetic Survey topographic map. The comparison appears good enough to justify further research in the refinement of radarclinometry as a technique for extracting topography from single radar images.

ROBERT L. WILDEY

Branch of Astrogeology,
U.S. Geological Survey, and
Department of Physics and Astronomy,
Northern Arizona University,
Flagstaff 86001

References and Notes

1. This is an adaptation of the term "photoclinometry" to radar. There is strong similarity in method. Fundamental papers in photoclinometry include the following: T. Rindfleisch, *Photogramm. Eng.* **32**, 262 (1966); K. Watson, *U.S. Geol. Surv. Prof. Pap. 599B* (1968); R. Wildey, *Icarus* **25**, 613 (1975).
2. Large expanses of undeveloped terrain that are homogeneous in normal radar backscatter are much more common than in the case of normal visual albedo [G. G. Schaber, G. L. Berlin, W. E. Brown, Jr., *Geol. Soc. Am. Bull.* **87**, 29 (1976)]. Knowledge of orbital position, range to surface, and nominal planetary radius establishes the incidence angle for the plane tangent to the surface. A calibration constant can be found that makes the average pixel value correspond to this angle.
3. The formal term equaling power per unit solid angle about a characteristic direction per unit area perpendicular to that direction is indicated; also called specific intensity or luminance, and directly proportional to backscattering cross-sectional density or the product of normal albedo and photometric function.
4. I do not mean to imply that pixel energy is directly proportional to specific intensity. If pixel energy is characterized by constant dwells in azimuth and range, then a proportionality factor can be shown to exist involving the product of the cotangent of the incidence angle and the secant of the projected angle, as seen from the radar, between the local normal and local vertical. Though a mathematical complication,

this effect increases the precision of practical radarclinometry.
5. A detailed mathematical theory is presented in R. L. Wildey, *Photogramm. Eng. Remote Sensing*, in press.
6. G. T. Ruck, D. E. Barrick, W. D. Stuart, C. K. Krichbaum, *Radar Cross-Section Handbook* (Plenum, New York, 1970), p. 757.
7. L. A. Soderblom, paper presented at the Radar Metrics Workshop, Jet Propulsion Laboratory, Pasadena, Calif., 1 September 1983. In fact, Soderblom stated that this correction, added to the production of subjective stereo imagery, was more important than the production of actual metric topography.
8. P. T. Eliason, L. A. Soderblom, P. S. Chavez, Jr., *Photogramm. Eng. Remote Sensing* **48**, 1571 (1981).
9. R. M. Batson, K. Edwards, E. M. Eliason, *J. Res. U.S. Geol. Surv.* **3**, 401 (1975).
10. ——, *Photogramm. Eng. Remote Sensing* **42**, 1279 (1975).

30 August 1983; accepted 15 February 1984

Gaseous Nitrate Radical: Possible Nighttime Atmospheric Sink for Biogenic Organic Compounds

Abstract. *The gaseous nitrate (NO_3) radical, which has recently been measured in nighttime ambient atmospheres over the United States and Europe at concentrations up to ~ 350 parts per trillion, has now been shown to react rapidly with the biogenically emitted organic compounds dimethyl sulfide (DMS), isoprene, and several monoterpenes. Computer simulations demonstrate that these reactions can dominate the atmospheric behavior of these organic compounds at night. Thus reaction with NO_3 radicals may be the unknown, nonphotochemical removal process for DMS recently invoked by Andreae and Raemdonck to explain the absence of a diurnal profile for DMS in maritime air influenced by continental air masses. Similarly, the nighttime reaction of NO_3 radicals with monoterpenes can be a dominant removal process, leading to very low monoterpene concentrations in ambient atmospheres during the early morning.*

The role of biogenically emitted organic compounds in the chemistry of both the polluted and the clean troposphere has received much attention (*1–5*). Sandberg *et al.* (*6*) and others (*7*) have proposed that hydrocarbons such as isoprene and the monoterpenes emitted from vegetation contribute significantly to photochemical air pollution, while dimethyl sulfide (DMS), emitted from oceans and other natural sources, is involved in the global atmospheric sulfur cycle (*8*), ultimately contributing to background acid deposition.

Current models of the atmospheric chemistry of organic compounds emitted from biogenic sources (*2, 9*) treat the consumption of such species as due solely to reaction with hydroxyl (OH) radicals or ozone (O_3) or to photolysis. However, serious discrepancies have been reported between the measured rates of emission from vegetation of isoprene and the monoterpenes and their observed ambient concentrations (*3, 4*). Moreover, Andreae and Raemdonck (*10*) have recently invoked an unknown, nonphotochemical removal process for DMS from "continentally influenced" marine air masses.

Within the past 3 years we and our collaborators (*11–14*) and Noxon and coworkers (*15*) have identified and measured the nitrate radical (NO_3) at night in both the clean and the polluted troposphere, using long pathlength (~ 1 to 17 km) differential optical absorption spectroscopy (DOAS). Recently, we have also measured the rate constants for the reaction in air of NO_3 radicals with a large number of organics (*16–18*) including DMS, isoprene, and selected monoterpenes. We report here calculations utilizing these kinetic and ambient concentration data, which show that nighttime reaction with the NO_3 radical is a dominant, previously unrecognized, atmospheric pathway for the removal of many organic compounds of biogenic origin.

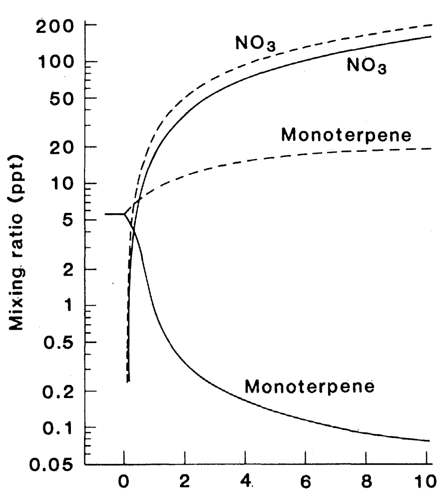

Fig. 1. Calculated time-concentration profiles for NO_3 radicals and monoterpenes for the Death Valley scenario (*21–24*). Solid lines are predictions for reaction between NO_3 radicals and monoterpenes; dashed lines are predictions for the assumption that there is no reaction.

Nighttime concentrations of NO_3 radicals measured in the United States (*11, 14*) and Europe (*13*) have ranged between the detection limit of the DOAS technique [~ 1 part per trillion (ppt)] and ~ 350 ppt, with typical concentrations in continental air masses ranging between ~ 10 and ~ 100 ppt. In polluted atmospheres the NO_3 radical concentrations increase (*11*) after sunset to a peak at ~ 2000 hours and then decrease rapidly to below the detection limit by about midnight. In contrast, in semiarid desert atmospheres the NO_3 radical concentrations generally increase (*14*) after sunset to a plateau value which persists until sunrise; after sunrise, the concentrations decline rapidly to less than 1 ppt because of the large photolytic cross section (*19*) of the NO_3 radical.

The rate constants (*20*) we have recently determined at room temperature for the gas-phase reactions of NO_3 radicals with biogenic organics are fast, ranging from ~ 5×10^{-13} cm^3 sec^{-1} per molecule for DMS (*17*) and isoprene (*18*) to (1 to 8) $\times 10^{-12}$ cm^3 sec^{-1} per molecule for the monoterpenes α- and β-pinene, *d*-limonene, and Δ^3-carene (*18*). To assess the importance of these reactions relative to reaction with OH radicals or with O_3, we have calculated the atmospheric lifetimes, τ, of DMS, isoprene, and selected monoterpenes for these three reaction pathways under two sets of atmospheric conditions (Table 1).

Reaction with NO_3 radicals is the dominant loss process for DMS and the monoterpenes, even under conditions corresponding to the clean troposphere (Table 1); for isoprene, consumption by NO_3 radicals at night is equal in importance to loss due to attack by OH radicals during daylight hours. In moderately polluted atmospheres, the reaction of NO_3 radicals with the monoterpenes leads to extremely short monoterpene lifetimes of ~ 1 to 5 minutes (Table 1). Indeed, the rate of *d*-limonene consumption by NO_3 radicals at night is about ten times that of reaction with O_3 and ~ 30 times that of daytime reaction with OH radicals. Clearly, reactions of NO_3 radicals with DMS, isoprene, and the monoterpenes significantly reduce the nighttime ambient concentrations of these organics relative to those that would occur if the NO_3 radical reactions are not considered, as is the case for current chemical models of the clean and polluted troposphere (*2, 3, 8, 9*).

In order to quantitatively illustrate the magnitude of the effects of these reactions, we have calculated NO_3 radical and monoterpene concentrations during nighttime hours, utilizing an appropriate